ACS OMEGA

http://pubs.acs.org/journal/acsodf

Article

High-Strength Epoxy Nanocomposites Reinforced with Photochemically Treated CNTs

Jae Won Lee, Sung-Soo Kim, Min Wook Lee, Jun Yeon Hwang, and Sook Young Moon*

Cite This: *ACS Omega* 2023, 8, 19789−19797

Read Online

ACCESS | Metrics & More | Article Recommendations | Supporting Information

ABSTRACT: A carbon nanotube (CNT)/epoxy nanocomposite was prepared using a photochemical surface modification process of CNTs. The vacuum ultraviolet (VUV)-excimer lamp treatment created reactive sites on the CNT surface. Increasing the irradiation time increased the oxygen functional groups and changed the oxygen bonding state such as C═O, C−O, and −COOH. By the VUV-excimer irradiation on CNTs, the epoxy infiltrated well between the CNT bundles and formed a strong chemical bond between CNT and epoxy. The tensile strength and elastic modulus of the nanocomposites with VUV-excimer irradiated sample during 30 min (R30) were found to increase by 30 and 68% compared to using pristine CNT, respectively. R30 was not pulled out and remained embedded in the matrix until the fracture occurred. The VUV-excimer irradiation is an effective surface modification and functionalization method for improving the mechanical properties of CNT nanocomposite materials.

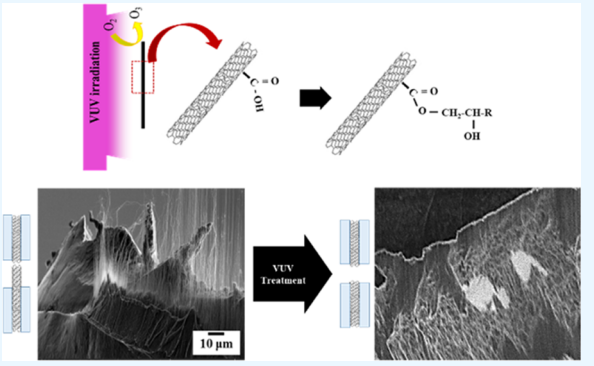

1. INTRODUCTION

Since carbon nanotubes (CNTs) were discovered, they have been studied for use as reinforcements in lightweight and high-performance composite materials because of their excellent physical properties.[1−5] CNTs have attracted attention as a potential material to replace carbon fiber because of their superior mechanical strength. However, it is difficult to exploit the properties of the individual CNTs in composite materials when using conventional fabrication processes because of several inherent issues, such as short aspect ratio, poor alignment, poor dispersing properties, and inert surface.

The low alignment and aspect ratio limit the commercial applications of CNTs. To overcome these issues, many researchers have focused on making orderly continuous CNT fibers. It is expected that materials having high mechanical, electrical, and thermal properties could be obtained by using well-oriented CNTs.[6−8] The well-aligned CNT fibers are predominantly produced via two different chemical vapor deposition (CVD) methods. First, the method of forest spinning process was researched by Zhang et al. in 2005.[9] This method is the most promising for use in the reinforcement of polymer composites because it shows high orientation and makes it possible to use them with a high volume fraction in composites. However, this method has a limitation for bulk-scale production because of dependence on substrate size. Alternatively, the direct spinning method is of particular interest to industrial applications because of scaled-up production.[10−12] The floating catalyst chemical vapor deposition (FC-CVD) process includes from catalyst formation to CNT aerogel formation, all steps occur within a few seconds. In this method, the aligned fiber and sheet are produced continuously at the end of a reactor. Although the alignment is inferior to that obtained using the forest spinning method, it is possible to manufacture fibers and sheets with improved orientation in bulk form by controlling the winding speed. The FC-CVD method is more appropriate for industrial applications.

On the other hand, CNTs are prone to agglomeration and entanglement within the matrix during composite fabrication due to their inert surface properties. Therefore, one possible method to improve the mechanical properties of composite applications is to activate the surface of the CNTs, thereby enhancing the interfacial bonding between CNT and the matrix. In most previous studies,[13−15] the functionalization of CNTs used harsh processes using strong acid mixtures. It generates the covalent bond with polymer, but these oxidation processes usually introduce defects on the graphitic layers. It limits the improvement of mechanical properties. The noncovalent functionalization of CNTs using polymer is an effective method to functionalize CNTs without structural defects.[16−20] However, it is difficult to maintain the alignment of CNTs due to the liquid-based processes. In addition, all

Received: March 7, 2023
Accepted: May 9, 2023
Published: May 23, 2023

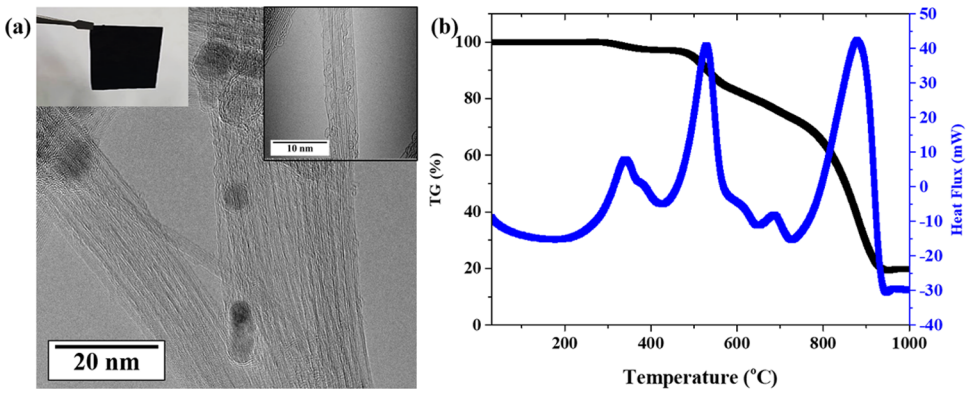

Figure 1. Synthesized pristine CNTs: (a) transmission electron microscopy (TEM) images and (b) thermogravimetric-differential scanning calorimetry (TG-DSC) of CNTs.

Scheme 1. Preparation of the CNT/Epoxy Composite

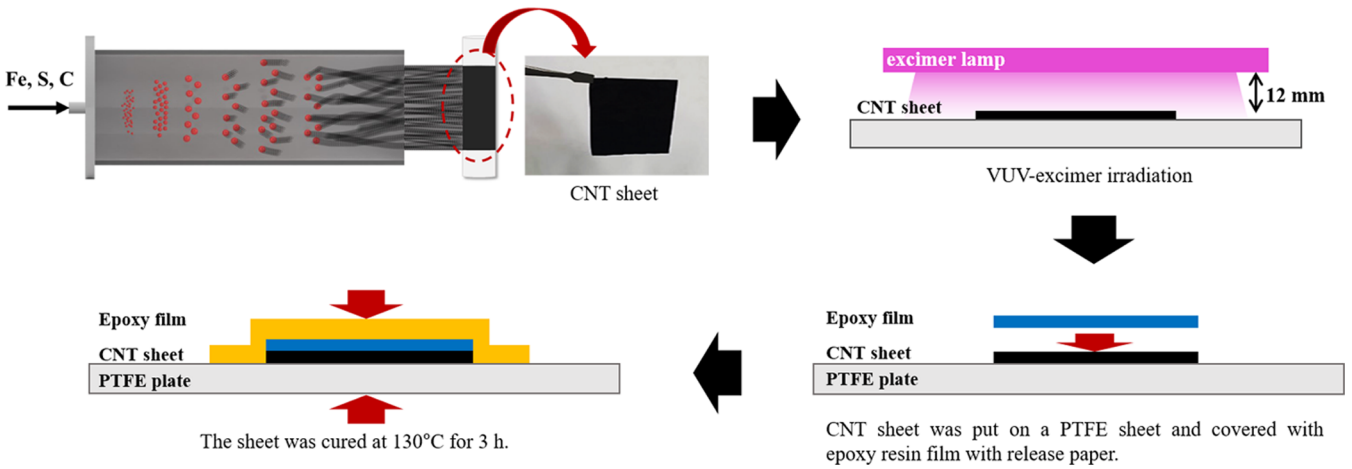

physical and chemical surface functionalization methods using chemical agents generate impurities on the CNT surfaces. These impurities are difficult to completely remove. Therefore, a very critical challenge remains regarding the development of an improved and more effective functionalization method.

Vacuum ultraviolet (VUV)-excimer irradiation is another approach for modifying the surface properties of carbon nanotubes (CNTs). VUV-excimer lamp has a wavelength range between 100 and 200 nm. The treatment can introduce various types of defects on the CNT surface, such as sp^3-hybridized carbon atoms and oxygen-containing functional groups, through the photochemical oxidation of the CNT surface.[21,22] However, there is no example of applying these VUV-excimer-treated samples to improve the properties of composite materials, and application review for future industrialization is required. In addition, it can be applied to various industrial fields as an element technology for manufacturing various types of composite structures.

In this study, we investigated an effective dry process for the surface modification of CNT surface through the VUV-excimer irradiation process while maintaining the alignment of CNTs. We report the surface modification of CNTs using VUV-excimer irradiation and develop a composite material using epoxy resin. The relationship between VUV-excimer irradiation and mechanical property improvement was investigated.

2. EXPERIMENTAL SECTION

2.1. Preparation of an Aligned CNT Sheet. The aligned CNT sheets were synthesized via the FC-CVD method (Figure 1a). The mixture of methanol (CH_3OH, Daejung Chemical, 99.8%) and *n*-hexane (C_6H_{14}, Daejung Chemical, 98.5%) in 9:1 vol % was used as a carbon source. Also, ferrocene (1 wt %, $Fe(C_5H_5)_2$, Sigma-Aldrich, 98%) and thiophene (3 vol %, C_4H_4S, Sigma-Aldrich, ≥99%) were added to the mixture as a catalyst and promoter, respectively. The prepared source solution was injected into the furnace at 1300 °C by a syringe pump at a rate of 12 mL/h. Hydrogen (H_2) and argon (Ar) were used as the carrier gases with 110:1 (vol %). The aerogel-like CNTs were synthesized and collected on a winder. The continuously synthesized CNT aerogel was collected and densified using acetone.

2.2. Surface Modification of CNT Sheets by the Photochemical Method. The surface modification of the CNT sheets was performed using an excimer lamp (VEX880W, Wonik QnC, Korea). The excimer lamp had a power density of 160 mW/cm^2, wavelength of 172 nm, and a high photon energy of 7.2 eV. The sheet was placed under a lamp and treated for a certain period of time in the air. The distance of the sample from the excimer lamp was fixed to be 12 mm. The exposure times used were 0, 10, 20, and 30 min, which we denote as Pristine (R0), R10, R20, and R30 in this work.

https://doi.org/10.1021/acsomega.3c01537
ACS Omega 2023, 8, 19789−19797

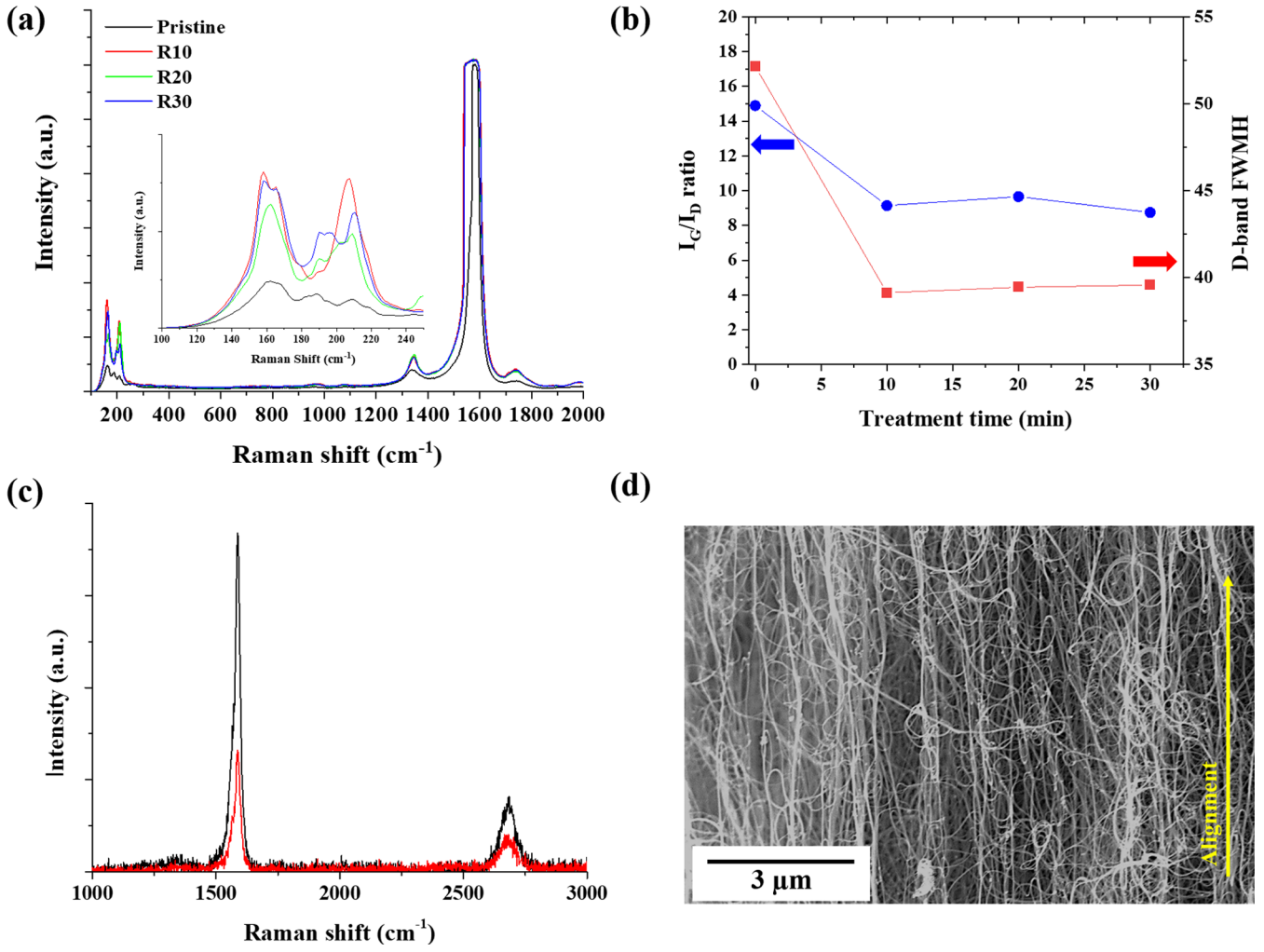

Figure 2. (a) Raman spectroscopy of CNT sheets with VUV-excimer irradiation (inset: radial breathing mode, RBM mode), (b) I_G/I_D ratio and D band FWMH, (c) $I_{G\parallel}/I_{G\perp}$ ratio of the alignment of CNT sheet, and (d) SEM images of the CNT sheet.

2.3. Preparation of CNT/Epoxy Nanocomposites. The nanocomposite film was prepared via the hot-press method. The CNT sheet (35 mm × 50 mm) was laid on a poly(tetrafluoroethylene) (PTFE) plate and covered with an uncured epoxy resin film (t = 50 μm, d = 54 g/m^2, Shinsung Comp. Materials). These films were cured at 130 °C for 3 h under a pressure of 3 MPa. In order to show the effect of the surface treatment of the CNTs on the mechanical properties of the nanocomposite, the content of the CNTs was minimized at 0.5 wt % (Scheme 1).

2.4. Characterization. The structure and morphology of CNTs and nanocomposites were characterized via Raman spectroscopy (via excited by a 514 nm laser, Renishaw, U.K.), transmission electron microscopy (TEM, Technai G2 F20, FEI), and field-emission scanning electron microscopy (FE-SEM, Verios 460, FEI). The TEM sample preparation was undertaken using focused ion beam scanning electron microscopy (FIB, Helios 650, FEI). The chemical properties of the surface of the CNTs after the VUV-excimer irradiation were characterized via Fourier transform infrared spectroscopy (FTIR, Nicolet iNTM10 infrared microscope, Thermo Fisher Scientific) and X-ray photoelectron spectroscopy (XPS, K-Alpha, Thermo Fisher Scientific). The thermodynamic reactions were analyzed through thermogravimetric-differential scanning calorimetry (TG-DSC, Labsys Evo, Setaram, France). The oxygen desorption progress was analyzed via mass spectroscopy (BGM202, Ulvac, Japan) using TG-DSC in a He atmosphere. The tensile strength of nanocomposite films was tested by a mechanical testing machine (model 5567A, Instron Corp.) using a displacement rate of 1 mm/min. The tensile test specimens were prepared according to ASTM638-14 and had a 25 mm gauge length. All samples were tested five times so that the results are reliable. The fracture dynamics were characterized via an in situ micro tensile test (2 kN, DEBEN UK Ltd., U.K.).

3. RESULTS AND DISCUSSION

Figure 1 shows the synthesized CNT sheets with a thickness of 10 μm. It consists of single-walled CNTs (SWCNTs) and few-walled CNTs (FWCNTs). The CNT diameters are mainly distributed between 1.5 and 3 nm. The synthesized CNT sheet had a purity of approximately 80%.

The CNT surface was functionalized using VUV-excimer irradiation using different treatment times without any chemical activating agent. The structural properties by irradiation treatment were investigated by Raman spectroscopy (Figure 2). All spectra show two Raman bands at 1346 and 1574 cm^{-1} between 1000 and 2000 cm^{-1}, assigned to the D band and G band, respectively. The G band is a collection of bands arising from the in-plane vibrational mode of carbon in

https://doi.org/10.1021/acsomega.3c01537
ACS Omega 2023, 8, 19789−19797

the graphite lattice, while the D band is produced by symmetric degradation effects such as defects or end tips or the presence of impurities such as catalyst particles or amorphous carbons.[23,24] The I_G/I_D ratio decreased from 14.89 to 8.74 with the increasing treatment time. The D band increased linearly with the VUV-excimer irradiation time, and the G band exhibited a broad shape. This may be due to the additional oxidation of the CNT surface. When the VUV-excimer irradiated in an atmosphere, light energy is consumed by the decomposition of oxygen in the atmosphere and ozone is generated. The difference between VUV-excimer irradiation and conventional UV-lamp treatment is that it can create ozone on the surface of the sample under being treated. The generated ozone is predicted to be chemisorbed on the CNT surface, and it can introduce various types of defects on the CNT surface, such as sp^3-hybridized carbon atoms and oxygen-containing functional groups. Because the free radical of atomic oxygen is actually attacking the C=C double bond.

Grujicic et al described the reaction of oxidation of CNTs by UV light via ab initio density functional theory (DFT) calculations.[25] O_2 molecules are very weakly bonded to the nanotube surface, but if the nanotubes are defective in their structure, they interact very strongly to form strong chemical bonds and result in significant charge transfer from the nanotubes to the O_2 molecules. In addition, UV-light excitation of the O_2 molecules can significantly reduce the activation energy for O_2 molecule chemisorption, thereby increasing the nanotube oxidation. Therefore, it can be seen that the ratio of I_G/I_D decreases because continuous VUV-excimer irradiation promotes oxidation of the surface and activates the surface.

The D-band FWHM of the pristine CNTs (Figure 2b) is 52 cm^{-1} and decreases to 39 cm^{-1} with VUV-excimer irradiation time, representing a reduction of carbon impurities such as amorphous carbon. The morphology of the CNT surface after VUV-excimer irradiation showed a cleaned and purified surface because of removed unreacted materials and amorphous carbon (Figure S1). However, as a result of the chemical adsorption of additional oxygen, highly reactive oxygen molecules reacted with the CNT structure to cause defects in the graphene layer. Therefore, the D-peak became sharp and the I_G/I_D ratio decreased. The radial breathing modes (RBMs) are used to calculate the tube diameters according to $d = 248/\omega_{RBM}$.[26] The calculated tube diameter distribution ranged from 1.2 to 1.5 nm, and it can be seen from the RBM data that the proportion of CNTs with a small increase in diameter. This is a phenomenon that occurs because the reactivity with UV light varies according to the chirality, surface state, and diameter of SWCNTs. The change in the SWCNT diameter with RBM due to UV irradiation will be dealt with in the next work.

In addition, the sheet alignment after treatment was studied via polarized Raman spectroscopy. The value of $I_{G\parallel}/I_{G\perp}$ of the G peak is used to determine the degree of alignment.[27] As a result of measuring the $I_{G\parallel}/I_{G\perp}$ value of the CNT sheet before and after treatment, the value of 2.8 did not change (Figure 2c). Although the CNT sheets are aligned to some extent, they are not perfectly aligned UD materials; therefore, when viewed under high magnification, there is a mix of misaligned areas (Figure S2). However, it can be seen from the polarized Raman results that the alignment is not broken by VUV-excimer irradiation. Therefore, it was confirmed that VUV-excimer irradiation is an effective method for surface treatment while maintaining the initial alignment of CNTs.

The surface modification of CNT by VUV-excimer irradiation was investigated by FTIR measurement. Figure 3

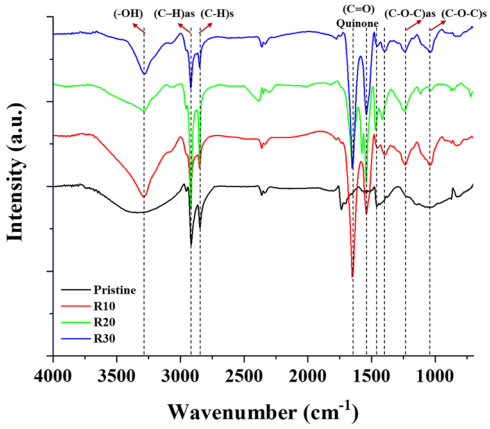

Figure 3. FTIR spectrum of pristine and VUV-excimer irradiation samples (Pristine, R10-30).

shows the IR spectra of pristine CNT and VUV-excimer irradiation samples (R10, R20, and R30). The increased oxygen-related functional groups, specifically ethers, epoxides, and carbonyls, were confirmed in VUV-excimer irradiation samples compared to pristine CNTs. The peaks at 1241 and 1041 cm^{-1} corresponded to asymmetric C−O−C and symmetric C−O−C stretching, respectively. The sharp peaks at 1650 and 1538 cm^{-1} are assigned to quinone groups (C=O) on the side walls of CNTs.[28] These functional groups, especially hydroxyl and carboxylic acid groups, allow CNTs to react with other surface groups. Thus, the more such functional groups, the stronger the bond with the matrix polymer can be formed.

The CNT surfaces were investigated through XPS to confirm the effect of the VUV-excimer irradiation (Figure 4). The peaks were analyzed using Gaussian peak fitting. The C 1s peaks show six peaks centered at 284.2, 284.7, 285.5, 287.9, 289.5, and 291 eV assigned to sp^2, sp^3, C−OH, C=O, O=C−O, and $\pi-\pi^*$, respectively (Figure 4).[29,30] The C−O and O=C−O ratio was increased with increasing treatment time. When the sample was processed for a long time (R30), an extra peak appeared at 289.5 eV, which can be assigned to the carboxyl group. This indicates that the CNT surface was well oxidized by the VUV-excimer irradiation. The oxygen-containing groups can also be confirmed in the O 1s peak (Figure S2). The carbonyl group (C=O) is present between 531 and 532 eV, the C−O bond of ether and hydroxyl is visible between 532 and 533.5 eV, and the ether oxygen atom of esters and hydrides is located between 533.8 and 534.6 eV.[31] All samples show the main two peaks at 532.4 and 533.4 eV corresponding to C−O/C−OH and O−C=O/C−O−C, respectively. The carbonyl group only exists in pristine CNTs. The VUV-excimer irradiation generates more C−O groups. Ozone oxidation of the CNT surface results in the formation of a Criegee's intermediate, followed by transformations leading to quinone, carbonyl, and lactone functional groups.[32,33] Therefore, it can be seen that the ratio of O−C=O/C−O−C increases again in the sample of R30 that has undergone the longest VUV-excimer irradiation. The peak of −COOH appeared only at R30, which is consistent with the result of the C 1s peak. In addition, as a result of analyzing the surface characteristics of the VUV irradiated surface and the

https://doi.org/10.1021/acsomega.3c01537
ACS Omega 2023, 8, 19789−19797

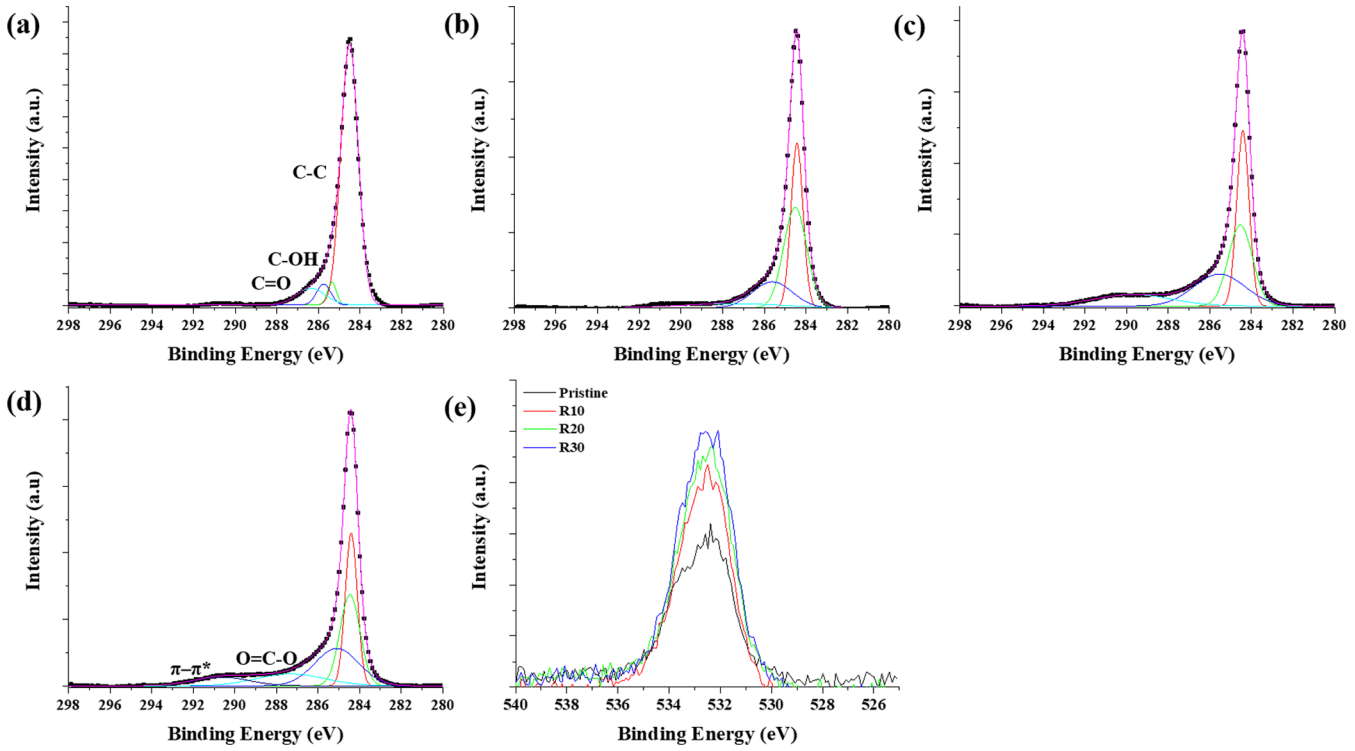

Figure 4. X-ray photoelectron spectroscopy of C 1s: (a) pristine CNT, (b) R10, (c) R20, (d) R30, and (e) O 1s.

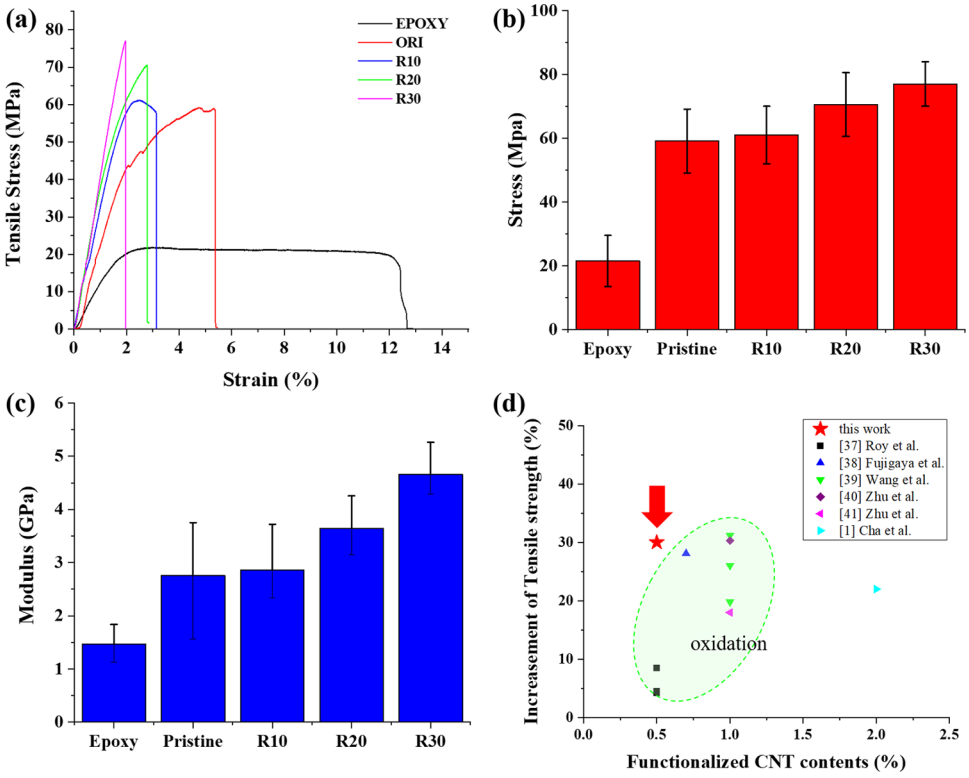

Figure 5. Mechanical properties of nanocomposite materials: (a) stress−strain curves, (b) tensile strength, (c) elastic modulus, and (d) stress−strain curve according to fiber direction.[37−41]

opposite surface (non-irradiated surface), it was confrimed that the non-irradicated surface was also sufficiently functionalized (Figure S3).

The temperature-programmed desorption (TPD) was analyzed in a He atmosphere for Pristine and R30 samples (Figure S4). It has been found that acidic oxygen-containing groups (e.g., carboxylic acid) and lactones and anhydrides are removed with the release of CO_2 at lower temperatures. On the other hand, phenol, anhydrous carbonyl, and neutral groups are more stable and release CO molecules at relatively

https://doi.org/10.1021/acsomega.3c01537
ACS Omega 2023, 8, 19789−19797

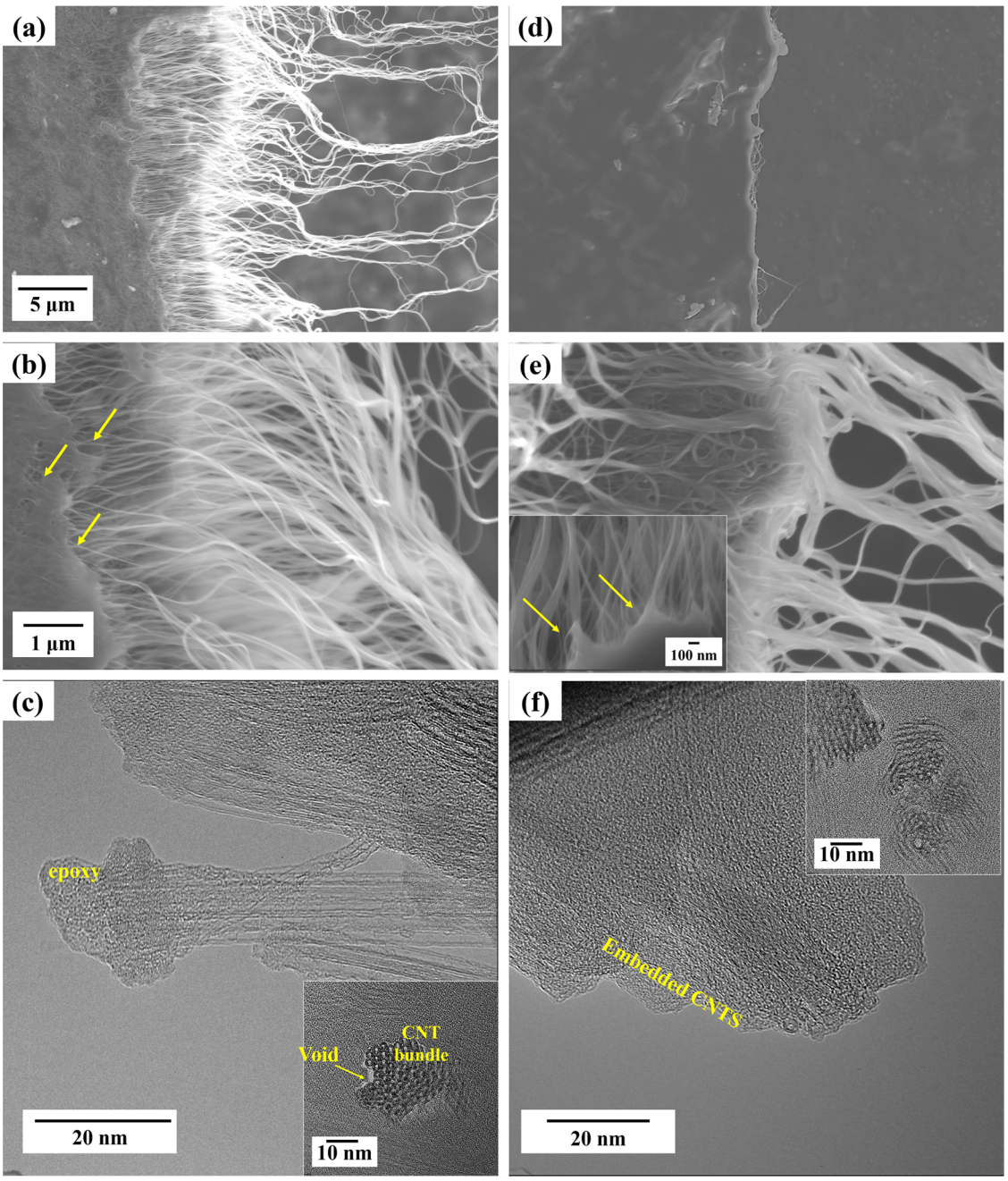

Figure 6. SEM and TEM images of the fractured surface of nanocomposite materials: (a)−(c) Pristine CNT/Epoxy and (d)−(f) R30/Epoxy material. [(c) and (f) inset: CNT bundle in the cross section of nanocomposite].

high temperatures.[31,34,35] The TPD data in pristine CNTs shows small quantities of CO_2 and CO compared to R30. These released CO_2 and CO were caused by impurities such as amorphous carbon generated in the CVD process. The VUV-excimer irradiation sample (R30) shows significantly different behavior from the pristine CNTs. This sample showed large amounts of CO_2 and CO emissions. CO_2 showed an initial release at about 250 °C and was released continuously. This is considered to be because the oxygen group derived from the carboxyl group on the surface of CNTs is released. R30 releases much higher amounts of CO compared to the initial CNTs. As can be seen from the results of XPS, it seems that this is because the bonding of C−O−C/O−C═O of ether or quinone released at high temperatures increases. The ozone in the VUV-excimer irradiation can create many oxygen-containing groups.[36] The thermal stability of CNTs with and without VUV-excimer irradiation was observed through DSC, which was analyzed in the air atmosphere. The oxidation and decomposition started at a lower temperature in the VUV-excimer-irradiated CNTs compared to pristine CNTs. The VUV-excimer irradiation creates large quantities of oxygen-containing groups and dangling bonds. Therefore, it can be confirmed that the VUV-excimer-exposed sample is more thermally unstable.

The nanocomposites with CNT sheets were prepared with epoxy resin. The mechanical properties of the nanocomposite with and without VUV-excimer irradiation of CNTs were investigated (Figure 5). Compared with the pristine CNT, the

https://doi.org/10.1021/acsomega.3c01537
ACS Omega 2023, 8, 19789−19797

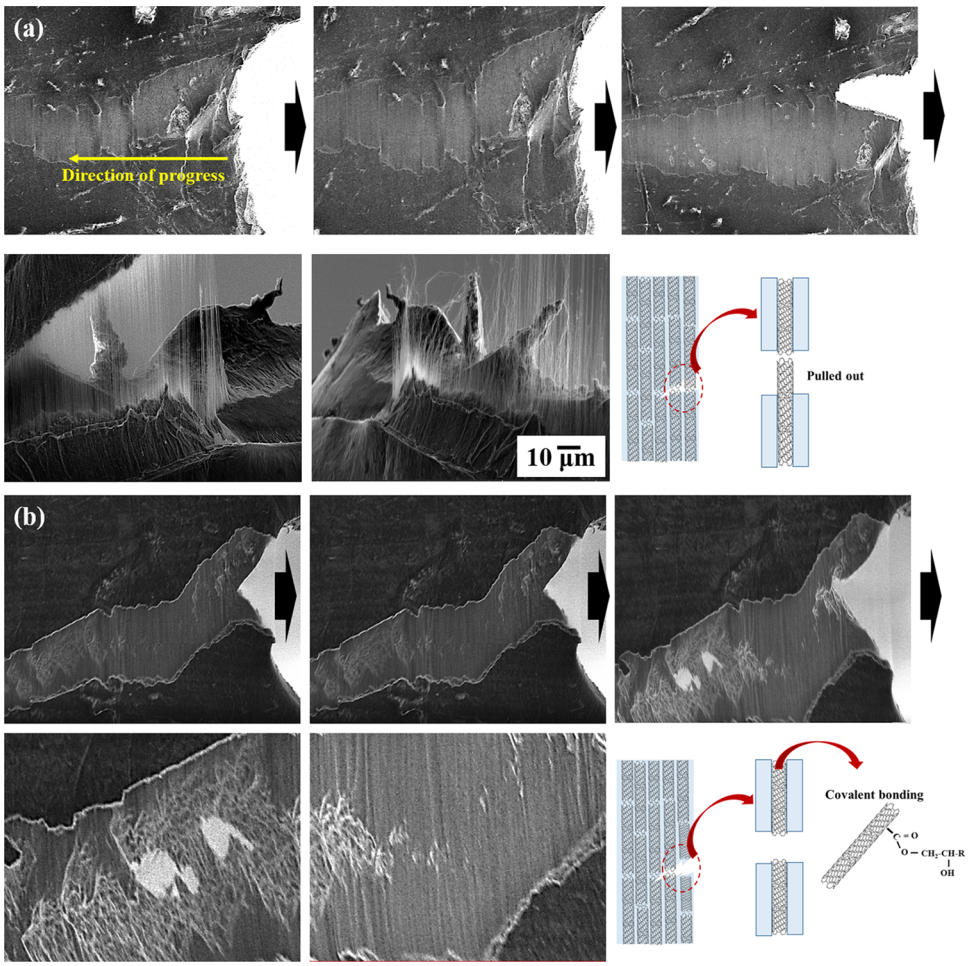

Figure 7. Fracture propagation in nanocomposites: (a) Pristine CNT/Epoxy and (b) R30/Epoxy.

observed improved tensile strength of the VUV-excimer-exposed CNT can be mainly attributed to the covalent cross-linking of the CNTs with epoxy. The degree of cross-linking increased with the increasing reaction time; this increased degree of cross-linking also increased the maximum fracture load of the CNT/epoxy nanocomposite. The tensile strength and elastic modulus of the pristine CNT/epoxy nanocomposite were 59.12 MPa and 2.76 GPa, respectively. Meanwhile, the tensile strength and elastic modulus of the R30 CNT/epoxy nanocomposite were increased to 77.02 MPa and 4.65 GPa, respectively. The tensile strength and elastic modulus of the nanocomposites were found to be increased by 30 and 68%, respectively. The elongation rate was found to decrease from 5.4 to 1.9%. Consequently, VUV-excimer irradiation is an effective method to functionalize the surface of CNTs and to improve the mechanical properties of the resultant nanocomposite. Figure 4d is a result of the comparison of the tensile strength increase rate according to the content of the functionalized CNTs in the low-wt % range. It can be seen that the high tensile strength increase rate was achieved with a lower content than other oxidized CNTs. Therefore, it can be confirmed that VUV-excimer irradiation is a very simple and effective method to functionalize the CNT surface and improve the bonding strength between the CNT and the polymer matrix.

The fracture surfaces of nanocomposites were examined using SEM and TEM (Figure 6). The fracture morphology was investigated to ascertain the load transfer properties of the sample. Many CNT bundles were pulled out from the nanocomposite and the CNT surfaces appeared clean, suggesting that the CNTs slipped in the epoxy resin under tensile loading (Figure 6a). A void was observed around the CNT bundles in the pristine CNT sample (Figure 6c inset). By contrast, the VUV-excimer-exposed samples (R30, Figure 6d) had only small quantities of CNT bundles drawn and the length of the CNTs pulled out across the fracture surface was short. It can be confirmed that the CNT surface is well covered with epoxy, and the visible voids around the fibers are not observed (Figure 6f). The quantity of individual CNT bundles at the fracture surface was much reduced in the VUV-excimer-exposed specimens. This is thought to be because the CNT sheet was uniformly impregnated with the epoxy resin and a strong chemical bond was formed with the CNT. Through this fracture morphology analysis, it can be inferred that the cross-linked CNTs are stressed and the uniformly distributed epoxy resin serves as a load transfer medium.

The in situ tensile test in the SEM and TEM setup was undertaken to investigate the fracture behavior characterization (Figure 7). In the case of the pristine CNT/epoxy nanocomposite sample (Figure 7a), the CNTs were easily pulled out as the test proceeded; the CNT slip phenomenon occurs from within the matrix. In the case of the VUV-excimer-exposed nanocomposite sample (Figure 7b), the interfacial bonding was well established by covalent cross-linking; thus,

https://doi.org/10.1021/acsomega.3c01537
ACS Omega 2023, 8, 19789−19797

the CNTs were not pulled out of the nanocomposite and instead remained embedded within the matrix until fracture occurred. It can therefore be concluded that VUV-excimer irradiation improves the mechanical properties of the nanocomposite material.

4. CONCLUSIONS

In summary, we have developed a facile method for the functionalization of CNTs using VUV-excimer irradiation. The VUV-excimer irradiation generates oxygen-containing functional groups. Increasing the treatment time increased the amount of numerous oxygen functional groups and changed the oxygen bonding state. We fabricated a CNT/epoxy nanocomposite via the hot-press method. The investigation of the fracture surface revealed excellent interfacial bonding with covalent cross-linking between the CNTs and the matrix resin. The tensile strength and elastic modulus of the R30 CNT/epoxy nanocomposites were found to be improved relative to the pristine CNT/epoxy nanocomposite. The tensile strength and elastic modulus of the nanocomposites with VUV-excimer irradiation were found to increase by 68 and 30% compared to pristine CNT, respectively. The fracture propagation shows different behavior of the samples with and without VUV-excimer irradiation. As a result of observing the fracture surface, many CNT bundles were pulled out from the nanocomposite made from pristine CNTs. By contrast, the nanocomposites constructed from CNTs that had been subject to the VUV-excimer irradiation showed good interfacial bonding; in this case, the CNTs were not pulled out and instead remained embedded in the matrix until the fracture occurred. We conclude that VUV-excimer irradiation is an effective method of improving the mechanical properties of nanocomposites.

■ ASSOCIATED CONTENT

Supporting Information

The Supporting Information is available free of charge at https://pubs.acs.org/doi/10.1021/acsomega.3c01537.

SEM images of CNT sheets (Figure S1); XPS spectra of O 1s of CNT sheet with various VUV-excimer irradiation time (Figure S2); XPS spectra of C 1s and O 1s of pristine and R30 CNT sheet (Figure S3); TG-DSC in air; TG-DTA in Ar; and TPD spectra in He (Figure S4) (PDF)

■ AUTHOR INFORMATION

Corresponding Author

Sook Young Moon − *Institute of Advanced Composite Materials, Korea Institute of Science and Technology (KIST), Wanju-gun, Jeonbuk 55324, Republic of Korea;* orcid.org/0000-0002-6102-6963; Email: moon.sookyoung@kist.re.kr

Authors

Jae Won Lee − *Institute of Advanced Composite Materials, Korea Institute of Science and Technology (KIST), Wanju-gun, Jeonbuk 55324, Republic of Korea; Department of Materials Science and Chemical Engineering, Hanyang University, Ansan-si, Gyeongi-do 15588, Republic of Korea*

Sung-Soo Kim − *Institute of Advanced Composite Materials, Korea Institute of Science and Technology (KIST), Wanju-gun, Jeonbuk 55324, Republic of Korea*

Min Wook Lee − *Institute of Advanced Composite Materials, Korea Institute of Science and Technology (KIST), Wanju-gun, Jeonbuk 55324, Republic of Korea;* orcid.org/0000-0003-3256-1067

Jun Yeon Hwang − *Institute of Advanced Composite Materials, Korea Institute of Science and Technology (KIST), Wanju-gun, Jeonbuk 55324, Republic of Korea*

Complete contact information is available at: https://pubs.acs.org/10.1021/acsomega.3c01537

Author Contributions

J.W.L. performed the experiment and formal analysis. S.-S.K. discussed the methodology and performed the formal analysis. M.W.L. discussed the methodology and investigation. J.Y.H. contributed to the reviewing and editing, project administration, and funding acquisition. S.Y.M. supervised and conceptualized the research and wrote, reviewed, and edited the manuscript.

Funding

This work was supported by the Korea Institute of Science and Technology (KIST) internal research program (2Z06901) and the Technology Development Program (S2940648) from the Ministry of SMEs and Startups (MSS, Korea).

Notes

The authors declare no competing financial interest.

■ REFERENCES

(1) Cha, J.; Jun, G. H.; Park, J. K.; Kim, J. C.; Ryu, H. J.; Hong, S. H. Improvement of modulus, strength and fracture toughness of CNT/Epoxy nanocomposites through the functionalization of carbon nanotubes. *Composites, Part B* **2017**, *129*, 169−179.

(2) Long, J. C.; Zhan, H.; Wu, G.; Zhang, Y.; Wang, J. N. High-strength carbon nanotube/epoxy resin composite film from a controllable cross-linking reaction. *Composites, Part A* **2021**, *146*, No. 106409.

(3) Ogasawara, T.; Tsuda, T.; Takeda, N. Stress-strain behavior of multi-walled carbon nanotube/PEEK composites. *Compos. Sci. Technol.* **2011**, *71*, 73−78.

(4) Wang, Q.; Wen, G.; Liu, L.; Zhu, B.; Su, D. Promising commercial reinforcement to the nanodiamond/epoxy composite by grafting ammonium ions. *J. Mater. Sci. Technol.* **2018**, *34*, 990−994.

(5) Guo, W.; Liu, C.; Sun, X.; Yang, Z.; Kia, H. G.; Peng, H. Aligned carbon nanotube/polymer composite fibers with improved mechanical strength and electrical conductivity. *J. Mater. Chem.* **2012**, *22*, 903−908.

(6) Kim, S. G.; Choi, G. M.; Jeong, H. D.; Lee, D.; Kim, S.; Ryu, K. H.; Lee, S.; Kim, J.; Hwang, J. Y.; Kim, N. D.; Kim, D. Y.; Lee, H. S.; Ku, B. C. Hierarchical structure control in solution spinning for strong and multifunctional carbon nanotube fibers. *Carbon* **2022**, *196*, 59−69.

(7) Koziol, K.; Vilatela, J.; Moisala, A.; Motta, M.; Cunniff, P.; Sennett, M.; Windle, A. High-Performance Carbon Nanotube Fiber. *Science* **2007**, *318*, 1892−1895.

(8) Jiang, C.; Saha, A.; Young, C. C.; Hashim, D. P.; Ramirez, C. E.; Ajayan, P. M.; Pasquali, M.; Martí, A. A. Macroscopic Nanotube Fibers Spun from Single-Walled Carbon Nanotube Polyelectrolytes. *ACS Nano* **2014**, *8*, 9107−9112.

(9) Zhang, M.; Fang, S.; Zakhidov, A. A.; Lee, S. B.; Aliev, A. E.; Williams, C. D.; Atkinson, K. R.; Baughman, R. H. Strong, transparent, multifunctional, carbon nanotube sheets. *Science* **2005**, *309*, 1215−1219.

(10) Zhang, Q.; Wei, N.; Laiho, P.; Kauppinen, E. I. Recent developments in single-walled carbon nanotubes thin films fabricated by dry floating catalyst chemical vapor deposition. *Top. Curr. Chem.* **2017**, *375*, 90.

(11) Yu, B.; Liu, C.; Hou, P. X.; Tian, Y.; Li, S.; Liu, B.; Li, F.; Kauppinen, E. I.; Cheng, H. M. Bulk Synthesis of Large Diameter Semiconducting Single-Walled Carbon Nanotubes by Oxygen-Assisted Floating Catalyst Chemical Vapor Deposition. *J. Am. Chem. Soc.* **2011**, *133*, 5232−5235.
(12) Lee, S. H.; Park, J.; Moon, S. Y.; Lee, S. Y.; Kim, S. M. Strong and Highly Conductive Carbon Nanotube Fibers as Conducting Wires for Wearable Electronics. *ACS Appl. Nano Mater.* **2021**, *4*, 3833−3842.
(13) Lavagna, L.; Bartoli, M.; Suarez-Riera, D.; Cagliero, D.; Musso, S.; Pavese, M. Oxidation of Carbon Nanotubes for Improving the Mechanical and Electrical Properties of Oil-Well Cement-Based Composites. *ACS Appl. Nano Mater.* **2022**, *5*, 6671−6678.
(14) Sun, Y. P.; Fu, K.; Lin, Y.; Huang, W. Functionalized carbon nanotubes: properties and applications. *Acc. Chem. Res.* **2002**, *35*, 1096−1104.
(15) Datsyuk, V.; Kalyva, M.; Papagelis, K.; Parthenios, J.; Tasis, D.; Siokou, A.; Kallitsis, I.; Galiotis, C. Chemical oxidation of multiwalled carbon nanotubes. *Carbon* **2008**, *46*, 833−840.
(16) Ghosh, A.; Rao, K. V.; Voggu, R.; George, S. J. Non-covalent functionalization, solubilization of graphene and single-walled carbon nanotubes with aromatic donor and acceptor molecules. *Chem. Phys. Lett.* **2010**, *488*, 198−201.
(17) Assali, M.; Leal, M. P.; Fernández, I.; Khiar, N. Synthesis and non-covalent functionalization of carbon nanotubes rings: new nanomaterials with lectin affinity. *Nanotechnology* **2013**, *24*, No. 085604.
(18) Usrey, M. L.; Strano, M. S. Controlling single-walled carbon nanotube surface adsorption with covalent and noncovalent functionalization. *J. Phys. Chem. C* **2009**, *113*, 12443−12453.
(19) Bilalis, P.; Katsigiannopoulos, D.; Avgeropoulos, A.; Sakellariou, G. Non-covalent functionalization of carbon nanotubes with polymers. *RSC Adv.* **2014**, *4*, 2911−2934.
(20) Dwyer, J. H.; Shen, Z.; Jinkins, K. R.; Wei, W.; Arnold, M. S.; Lehn, R. C. V.; Gopalan, P. Solvent-Mediated Affinity of Polymer-Wrapped Single-Walled Carbon Nanotubes for Chemically Modified Surfaces. *Langmuir* **2019**, *35*, 12492−12500.
(21) Vosmanská, V.; Barb, R. A.; Kolarva, K.; Rimpelova, S.; Heitz, J.; Svorcik, V. Effect of VUV-excimer lamp treatment on cellulose fiber. *Int. J. Polym. Anal. Charact.* **2016**, *21*, 337−347.
(22) Amiri, Z.; Moussavi, G.; Mohammadi, S.; Giannakis, S. Development of a VUV-UVC/peroxymonosulfate, continuous-flow Advanced Oxidation Process for surface water disinfection and Natural Organic Matter elimination: Application and mechanistic aspects. *J. Hazard. Mater.* **2021**, *408*, No. 124634.
(23) Jorio, A.; Saito, R.; Hafner, J. H.; Lieber, C. M.; Hunter, M.; Hunter, M.; McClure, T.; McClure, T.; Dresselhaus, G.; Dresselhaus, M. S. Structural (*n*,*m*) determination of isolated single-wall carbon nanotubes by resonant Raman scattering. *Phys. Rev. Lett.* **2001**, *86*, 1118−1121.
(24) Yan, X.; Itoh, T.; Kitahama, Y.; Suzuki, T.; Sato, H.; Miyake, T.; Ozaki, Y. A Raman Spectroscopy Study on Single-Wall Carbon Nanotube/Polystyrene Nanocomposites: Mechanical Compression Transferred from the Polymer to Single-Wall Carbon Nanotubes. *J. Phys. Chem. C* **2012**, *116*, 17897−17903.
(25) Grujicic, M.; Caoa, G.; Raob, A. M.; Trittb, T. M.; Nayak, S. UV-light enhanced oxidation of carbon nanotubes. *Appl. Surf. Sci.* **2003**, *214*, 289−303.
(26) Dillon, A. C.; Yudasaka, M.; Dresselhaus, M. S. Employing Raman Spectroscopy to Qualitatively Evaluate the Purity of Carbon Single-Wall Nanotube Materials. *J. Nanosci. Nanotechnol.* **2004**, *4*, 691−703.
(27) Koziol, K.; Vilatela, J.; Moisala, A.; Motta, M.; Cunniff, P.; Sennett, M.; Windle, A. High performance carbon nanotube fiber. *Science* **2007**, *318*, 1892−1895.
(28) Kuznetsova, A.; Mawhinney, D. B.; Naumenko, V.; Yates, J. T.; Liu, J.; Smalley, R. E. Enhancement of adsorption inside of single walled nanotubes opening the entry ports. *Chem. Phys. Lett.* **2000**, *321*, 292−296.
(29) Hou, P. X.; Xu, S. T.; Ying, Z.; Yang, Q. H.; Liu, C.; Cheng, H. M. Hydrogen adsorption/desorption behavior of multi-walled carbon nanotubes with different diameters. *Carbon* **2003**, *41*, 2471−2476.
(30) Okpalugo, T. I. T.; Papakonstantinou, P.; Murphy, H.; McLaughlin, J.; Brown, N. M. D. High resolution XPS characterization of chemical functionalized MWCNTs and SWCNTs. *Carbon* **2005**, *43*, 153−161.
(31) Larciprete, R.; Gardonio, S.; Pettaccia, L.; Lizzit, S. Atomic oxygen functionalization of double walled C nanotubes. *Carbon* **2009**, *47*, 2579−2589.
(32) Criegee, R. Mechanism of ozonolysis. *Angew. Chem., Int. Ed.* **1975**, *14*, 745−752.
(33) Simmons, J. M.; Nichols, B. M.; Baker, S. E.; Marcus, M. S.; Castellini, O. M.; Lee, C. S.; Hamers, R. J.; Eriksson, M. A. Effect of ozone oxidation on single-walled carbon nanotubes. *J. Phys. Chem. B* **2006**, *110*, 7113−7118.
(34) Haydar, S.; Moreno-Castilla, C.; Ferro-García, M. A.; Carrasco-Marín, F.; Rivera-Utrilla, J.; Perrard, A.; Joly, J. P. Regularities in the temperature-programmed desorption spectra of CO_2 and CO from activated carbons. *Carbon* **2000**, *38*, 1297−1308.
(35) Figueiredo, J. L.; Pereira, M.F.R.; Freitas, M.M.A.; Órfão, J.J.M. Characterization of active sites on carbon catalysts. *Ind. Eng. Chem. Res.* **2007**, *46*, 4110−4115.
(36) Schönherr, J.; Buchheim, J.; Scholz, P.; Stelter, M. Oxidation of carbon nanotubes with ozone and hydroxyl radicals. *Carbon* **2017**, *111*, 631−640.
(37) Roy, S.; Petrova, R. S.; Mitra, S. Effect of carbon nanotube (CNT) functionalization in epoxy-CNT composites. *Nanotechnol. Rev.* **2018**, *7*, 475−485.
(38) Fujigaya, T.; Saegusa, Y.; Momota, S.; Uda, N.; Nakashima, N. Interfacial engineering of epoxy/carbon nanotubes using reactive glue for effective reinforcement of the composite. *Polym. J.* **2016**, *48*, 183−188.
(39) Wang, Q.; Shi, W.; Zhu, B.; Su, D. S. An effective and green $H_2O_2/H_2O/O_3$ oxidation method for carbon nanotube to reinforce epoxy resin. *J. Mater. Sci. Technol.* **2020**, *40*, 24−30.
(40) Zhu, J.; Peng, H.; Rodriguez-Macias, F.; Margrave, J. L.; Khabashesku, V. N.; Imam, A. M.; Lozano, K.; Barrera, E. V. Reinforcing Epoxy Polymer Composites Through Covalent Integration of Functionalized Nanotubes. *Adv. Funct. Mater.* **2004**, *14*, 643−648.
(41) Zhu, J.; Kim, J.; Peng, H.; Margrave, J. L.; Khabashesku, V. N.; Barrera, E. V. Improving the dispersion and integration of single-walled carbon nanotubes in epoxy composites through functionalization. *Nano Lett.* **2003**, *3*, 1107−13.

https://doi.org/10.1021/acsomega.3c01537
ACS Omega 2023, 8, 19789−19797